Ablative collision avoidance for space debris in the Low Earth Orbit by a single multi-kJ pulse from a ground-based laser

Stefan Scharring, Gerd Wagner, Jürgen Kästel, Wolfgang Riede, Jochen Speiser
German Aerospace Center (DLR), Institute of Technical Physics, Pfaffenwaldring 38-40, 70569 Stuttgart, Germany

ABSTRACT

We analyze the conceptual idea whether already a single high energy laser pulse, emitted from a laser station on ground, might cause material ablation at the surface of a debris object generating recoil for a sufficiently high velocity change to allow for space debris collision avoidance.

In our simulations we assess the effects of atmospheric constraints like laser power loss due to aerosol extinction as well as laser beam broadening and pointing jitter as a result from atmospheric turbulence. For the compensation of turbulence, the usage of adaptive optics is explored in terms of a suitable transmitter configuration in combination with a laser guide star. Based on the ESA DISCOS catalogue, virtual targets with simplified geometric shapes are employed to investigate laser-matter-interaction with rocket bodies, mission-related objects and inactive payloads. In addition, the NASA Standard Breakup Model serves as a reference for fragments from collisions and explosions yielding an ensemble of 9101 debris targets in the Low Earth Orbit. For these objects, a study on laser-ablative recoil is carried out using a raytracing-based code considering both the unknown target orientation as well as residual laser pointing errors constituting sources of randomness in overall 5 dimensions (3 rotational, 2 translational) which are addressed in a Monte Carlo approach. Laser momentum coupling is calculated for the computed laser fluence distribution at the mean altitude of the particular debris object. As input for the calculation of laser-matter interaction, experimental data from the irradiation of aluminum, copper, and steel as representative space debris materials are employed.

The simulation results on laser-imparted momentum are discussed in terms of irradiation elevation angle, displacement on the orbital trajectory, momentum transfer uncertainty, success probability, debris material and limitations due to debris size, mass, and the required minimum fluence for the initiation of a laser ablation process.

1. INTRODUCTION

Due to the increasing amount of space debris and driven by the lack off its accessibility for orbit modification, several laser-based concepts for remote momentum transfer (MT) to space debris have been proposed in the recent years [1][2]. In particular, MT via photon pressure appears to become feasible, due to the commercial availability of continuously emitting (CW) lasers with an average power output beyond the 10 kW level. For the purpose of space debris collision avoidance, simulations have already shown that sufficiently high velocity increments of a few mm/s can be achieved by target irradiation during several laser station transits [1]. Feasibility and estimated performance of corresponding laser station networks for debris tracking and collision avoidance have been investigated recently in the study LARAMOTIONS (Laser Ranging and Momentum Transfer systems evolution Study). The study had been carried out by a consortium under the lead of our institute as a conceptual analysis for the European Space Agency (ESA). An overview over the study results is given in [3] while a detailed astrodynamics feasibility study of orbital collision avoidance using photon pressure is lined out in [4] whereas detailed results on the employed laser station networks are shown in [5].

Momentum coupling from laser ablation exceeds coupling by photon pressure by 3 to 5 orders of magnitude [6]. Therefore, ablation is typically discussed as a suitable mechanism for laser-based debris removal by perigee lowering during multiple high energy laser station transits. Recent drop experiments in vacuum with a few-centimeters sized targets have shown, however, the great potential of laser-ablative momentum transfer for space debris collision avoidance proving that already a *single* laser pulse might induce a velocity change Δv of several tens of cm/s to a small space debris-like object [7].

Support by these findings we have performed an internal study named PARAMOTIONS (Pulsed Ablative Remote Advanced Motion Study, following the abovementioned ESA project) in order to explore the potential of laser ablation for collision avoidance. In this study, only a single laser station is employed for momentum transfer instead of a laser station network. Moreover, we restrain the laser-based maneuver for collision avoidance to a single station pass of debris object and analyze the question whether it would to be sufficient to even employ only a single high energy laser pulse during this station transit.

2. FUNDAMENTALS

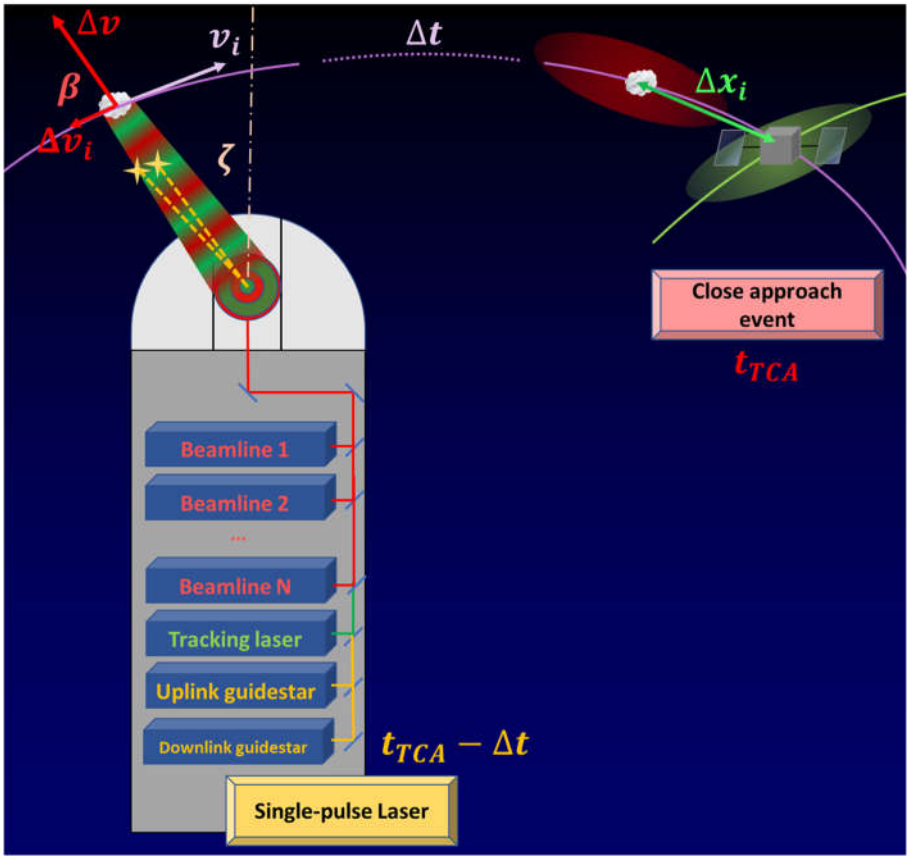

Figure 1. Conceptual view of laser-based collision avoidance using a ground station operating at a point time Δt before the time of closest approach t_{TCA}. Laser power beaming is assisted by adaptive optics and laser ranging. Laser-induced momentum causes a decrement Δv_i in the in-track velocity of the debris object yielding a displacement Δx_i on its trajectory at the time of closest approach that enables collision avoidance. The objects' covariances are indicated by the ellipsoids shown in the close approach event.

A scheme of debris collision avoidance by a ground-based laser is shown in Figure 1. Via the high energy laser pulse, momentum is exerted to the debris object. Projection on the tangent of the trajectory using $\cos\beta$ gives the in-track velocity decrement Δv_i by which the target is decelerated in order to achieve a sufficient displacement Δx_i between the conjunction partners at the time t_{TCA} of closest approach. Note that in advance it has to be derived from orbit propagation whether acceleration would be more beneficial than deceleration of the object. If so, the target has to be irradiated during the descending phase of its station pass instead.

Unlike force induced from laser photon pressure, the amount of imparted momentum from laser ablation does not scale linear with laser power, but exhibits a strongly non-linear dependency from the applied laser fluence Φ. Moreover, dependencies on both laser parameters as well as the targeted material exist. Therefore, it has to be analyzed how a large laser fluence can be achieved at the target position which is sufficient to yield the desired target displacement. Apparently, this has to be addressed by an appropriately high laser pulse energy E_L, which is

one of the target parameters of our study. But on top of that, with the fluence $\Phi = E_{in}/A_s$ being the ratio of transmitted laser energy E_{in} to the laser spot area A_s, the laser beam quality, quantified by the beam quality parameter M^2, rules the spot size that can be achieved by focusing the beam to the target, together with the distance z to the target, depending on orbit altitude h and the zenith angle ζ of beam pointing. On the other hand, the usable fraction of momentum Δv_i depends from the projection angle of the line-of-sight onto the trajectory, which in turn is a function of the beam pointing angle ζ as well.

Therefore, the laser irradiation maneuver has to be thoughtfully configured in order to maximize the debris displacement and to minimize the residual risk of collision. For a quantitative assessment of such a maneuver and, thus, the feasibility of laser-based collision avoidance (CA), different criteria are possible. It is a typical approach to assess whether the collision probability of the analyzed event can be decreased to fall below the accepted collision probability level (ACPL), usually $p_{ACPL} = 10^{-4}$ when accurate orbital data is available [8]. Whereas this figure of merit requires covariance determination from orbit propagation, we restrain here to a simplistic approach focusing solely on the in-track displacement of the target on its trajectory due to the imparted in-track velocity decrement.

For the altitude range of $h \in [579\ km; 1179\ km]$ considered in this study, see below, it can be deduced from the Hohmann transfer relations for a circular orbit that the in-track displacement Δx_i resulting from an instantaneous velocity change of $\Delta v_i = 1\ mm/s$ amounts to $\Delta x_i = 259.2\ m$ after a timespan of $\Delta t = 24\ h$ from the point in time where the velocity change took place. Note that Δx_i scales linearly with Δv_i and Δt. Assuming for the sake of simplicity that the laser-based CA maneuver takes place $\Delta t_{TCA} = 24\ h$ prior to the time t_{TCA} of closest approach (TCA), different feasibility criteria for laser-based CA can be used as requirements for successful CA:

1. $\Delta x_i \geq X$ where X is the maximum target extension yielding $\Delta v_{dim} \geq 1\ mm/s \cdot X/259.2\ m$ as a feasibility criterion which gives a target-specific Δv_{dim} which depends from the target dimensions. This criterion simply represents the requirement to shift an object by its own maximum extension X. In reality, however, this is not likely to be a reasonable criterion for successful CA since it would require exact knowledge of the target position. Instead, uncertainty stemming from target observations has to be considered.
2. $\Delta x \geq 2 \cdot \sigma_{i,LT} = 25.92\ m \rightarrow \Delta v \geq \Delta v_{LT,0} := 0.1\ mm/s$. This threshold refers to an earlier feasibility study on debris nudging using laser photon pressure as lined out in greater detail in [3]. There, we assumed a very high precision in knowledge of the debris position from frequent laser tracking. Furthermore, we considered 10 laser irradiations during a time span of 48 h before TCA to achieve this criterion, reducing the required velocity decrement down to $\Delta v_{LTpp} := 0.01\ mm/s$. In fact, it turned out in the later course of the study that this preliminary assessment for the in-track uncertainty is very close to the average in-track uncertainty directly after a laser tracking $\sigma_{i,LT} = 21.8\ m$ as reported in [5].
3. $\Delta x \geq 2 \cdot \sigma_{i,LXN} = 414.4\ m \rightarrow \Delta v \geq \Delta v_{LXN} := 1.6\ mm/s$. The value of $\sigma_{i,LXN} = 207.2\ m$ represents the average in-track uncertainty in a small-sized global laser ranging network comprising 5 European + 4 overseas stations (denoted as large extended network (LXN) in [5]).
4. It has to be noted that the abovementioned thresholds, Δv_{dim}, $\Delta v_{LT,0}$, and Δv_{LXN}, rely on knowledge about the target position at t_{TCA} which is not available by $\Delta t_{TCA} = 24\ h$ in advance – even not with the named laser ranging network LXN, where laser ranging measurements are carried out several times per day in order to achieve the small average covariance $\sigma_{i,LXN}$ of propagated orbital data. If, instead, laser tracking is carried out $\Delta t_{TCA} = 24\ h$ prior to t_{TCA} without any further measurements until the laser-based CA maneuver is carried out, the in-track covariance of orbital data after 24 h propagation has to be considered. From our computations in [3],[5] on covariance evolution regarding the ability of "blind" laser tracking, i.e., without target re-acquisition, we have found that this uncertainty is rather large, ranging from $\sigma_i = 305\ m$ at $h = 1180\ km$ up to $\sigma_i = 692\ m$ at $h = 580\ km$, which is comparable to covariances from radar observations. Here, we introduce the altitude-dependent thresholds of $\Delta v_{LT,24}^{(\sigma)}(h)$ and $\Delta v_{LT,24}^{(2\sigma)}(h)$ denoting the required velocity change to yield an in-track displacement that exceeds σ_i and $2\sigma_i$, respectively.

In sum, it can clearly be seen that the feasibility of collision avoidance is closely related to the associated uncertainty in debris observations, constituting a trade-off between measurement and momentum transfer. Therefore, the success probability of laser-ablative collision avoidance is assessed in our simulations using all five proposed feasibility criteria, i.e., $\Delta v_{dim}, \Delta v_{LT,0}, \Delta v_{LXN}, \Delta v_{LT,24}^{(\sigma)}$ and $\Delta v_{LT,24}^{(2\sigma)}$.

3. STUDY SETTINGS

3.1 Laser station

Already 25 years ago, C. Phipps proposed in his pioneering paper [9] on ground-based laser debris removal the usage of a laser with pulse energies of $E_L = 15\ kJ$ at a pulse repetition rate of $f_{rep} = 2\ Hz$ for the removal of space debris from the Low Earth Orbit (LEO) by extreme target deceleration using a large number of laser pulses. Later on, A. Rubenchik concretized this approach discussing the usage of laser beamlines like those used for ignition of inertial confinement fusion at the National Ignition Facility (NIF) at Lawrence Livermore National Laboratory (LLNL) for debris removal [10]. Laser parameters have matched Phipps' concept quite well: The pulse energy of such a beamline amounts to $E_L = 19\ kJ$, operating at a wavelength of $\lambda = 1053\ nm$ with a pulse duration of $\tau = 5\ ns$ [11]. The pulse repetition rate, however, restricted to a few laser pulses per day, is far too poor for this purpose, unless all 192 available beamlines would be fired in a pulse series one after the other. For our scope of collision avoidance with a single laser pulse, however, such a beamline appears to be suitable and is considered as the baseline configuration in our simulations. Note that only few comparable laser systems already exist worldwide, among them the Laser Mégajoule in France operating at $E_L = 18\ kJ$, $\lambda = 1053\ nm$ with pulse durations of in the range of a few hundred picoseconds up to $\tau = 25\ ns$ [12].

Large aperture transmitters had been proposed in the past for ground-based laser operations with space debris, e.g., $D_T = 6\ m$ in [9]. To allow for comparison with the findings from our recent study LARAMOTIONS on CA by photon pressure [3], we have chosen a significantly smaller transmitter aperture, $D_T = 2.5\ m$. Regarding the laser beam quality, however, we deviated from the settings in [3] assuming a laser beam quality parameter of $M^2 = 2.25$ to account for the rectangular beam profile of the NIF beamlines, whereas $M^2 = 1.5$ was employed for the CW lasers of LARAMOTIONS.

The combination of small debris size (in the meter range) and large distances between debris and laser station (up to thousands of kilometers) demands for focusing of the laser beam to the target's position. Dynamic adjustment of the telescope's focal length can be carried out using real-time data from laser ranging to the object, carried out simultaneously from the same laser site. Moreover, if adaptive optics is used in downlink, laser tracking could provide a position uncertainty as low as $\sigma_t = 0.1\ arcsec$ [3], which is essential for the required pointing accuracy of the high energy laser beam.

3.2 Debris Targets

For the space debris target population, the operational orbital regime (OOR) which had been proposed by ESA for the LARAMOTIONS study [3] is used comprising integer targets, such as 606 rocket bodies, 770 payloads, and 90 mission-related objects, as well as not less than 7636 debris fragments. These objects are located on orbits with a semi-major axis length between 6950 km and 7550 km together with a numerical eccentricity between 0 and 0.2 (as of July 2, 2019). Moreover, to ensure accessibility over Europe mainland, an inclination interval from 65° up to 115° has been set. Orbital data have been taken from the USSTRATCOM catalogue.

For a detailed modeling of laser-debris interaction, we have used information on mass m, cross-sectional area A_{cs} (optical) and A_{rcs} (radar), geometric shape and dimensions X, Y, Z where available from ESA's DISCOS database. Moreover, a statistical description of the debris fragment population as of ESA's MASTER-8 model was employed. Depending on the data on debris category, shape and dimensions, the debris targets have been modeled as individual simple geometries (cube, box, sphere, ellipsoid, cylinder etc.), cf. [3] for more details.

3.3 Laser-ablative Momentum

Due to their high abundance in the space debris population [13], aluminum, stainless steel, and copper have been selected as sample debris surface materials for our simulations. Experimental data for the momentum coupling coefficient $c_m = \Delta p / E_T$, as the ratio of imparted momentum Δp to absorbed laser pulse energy E_T, has been extracted from [14]. This data has been fitted using the empirical function

$$c_m(\Phi) \approx \frac{\Phi - \Phi_0}{a + \Phi - \Phi_0} \cdot b \cdot 12.46 \cdot A^{7/16} \cdot \left(\frac{\sqrt{\tau}}{10^{-4} \cdot \lambda \cdot \Phi} \right)^c \quad (1)$$

from [15] where A is the atomic mass of the target material, λ is the laser wavelength, τ denotes the laser pulse length, Φ represents the laser fluence at the target surface, Φ_0 is the threshold fluence for laser ablation, and a, b, c are fit parameters related to increase, peak, and subsequent decrease of $c_m(\Phi)$ with increasing fluence. The corresponding datafits are shown in Fig. 2. Note that the decrease of c_m with higher fluences does not mean a lower imparted momentum Δp but points to the diminished efficiency of momentum coupling, as c_m can be understood as a rather technical figure of merit similar to a thrust-to-power ratio.

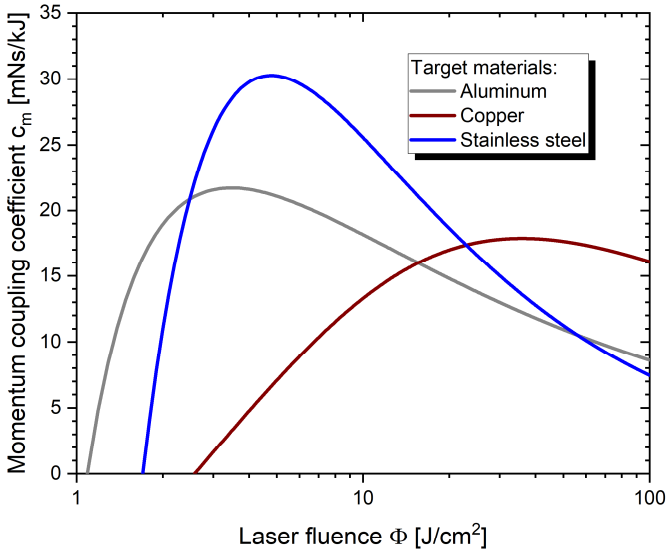

Fig. 2. Momentum coupling coefficient for recoil from laser ablation at a target surface under pulsed irradiation. Laser parameters: $\lambda = 1064\ nm, \tau = 5\ ns$.

Table 1. Parameters used in Eq. 1 for simulation of momentum coupling by laser ablation, cf. Fig. 2.

Material	$a\ [J/cm^2]$	$b\ [mNs/kJ]$	$c\ [-]$	$\Phi_0\ [J/cm^2]$	$A\ [amu]$
Aluminum	0.77187	0.19058	0.35657	1.08969	26.98
Copper	12.89351	0.26866	0.30087	2.57905	63.55
Stainless steel	2.05827	0.1367	0.62214	1.70157	54.84

3.4 Numerical Method

For the computation of laser-induced momentum from material ablation we employed the DLR code EXPEDIT (Examination Program for Irregularly Shaped Debris Targets). This highly parallelized code is based on raytracing, which allows to compute momentum rising from a laser spot with an, e.g., Gaussian intensity profile $\Phi(\vec{r})$ onto an arbitrarily shaped target. For this purpose, the infinitesimal momenta dp exerted to target surface elements of the area dA are computed using $dp = c_m\big(\Phi(\vec{r})\big) \cdot \Phi(\vec{r}) \cdot dA$, cf. [15] for more details on this numerical discretization of laser-matter interaction. Then, using Eq. 1, the imparted momentum can be obtained from integration over the irradiated target surface employing the fit parameters shown in Table 1.

4. FEASIBILITY ANALYSIS

4.1 Laser Fluence

For a first assessment about nudging feasibility the radius r_s of the focused laser spot has been computed as a function of the object altitude and zenith angle following [16]

$$\boldsymbol{r_{s,vac} = \frac{M^2 \lambda\, z(\zeta, h)}{\pi\, w_0}} \tag{2}$$

where M^2 is the laser beam quality parameter, λ the laser wavelength, $w_0 = 0.715 \cdot D_T/2$ the beam waist given by the telescope aperture diameter D_T, and z is the distance from the transmitter to the debris target at an orbital altitude h, irradiated under a zenith angle ζ. Then, the average fluence in orbit can be derived from the laser energy E_{in} arriving at the debris position using $\langle\Phi\rangle = E_{in}/(\pi r_s^2)$, cf. Fig. 3. It has to be noted, however, that the results from Eq. 2, depicted in Fig. 3a), only reflect the case of vacuum beam propagation. In reality, the impact of atmospheric extinction and turbulence has to be considered. Hence, for a more realistic computation extinction has been incorporated assuming $T = \exp(-AOD \cdot \sec\zeta)$ for the atmospheric transmission where the aerosol optical depth AOD for the used wavelength is set to $AOD = 0.144$ in agreement with the findings from [17]. Moreover, from geometric considerations on outshining losses at the transmitter a transmission efficiency of $\eta_T = 98\%$ has been derived giving the fraction of laser pulse energy E_{in} arriving at the debris position according to $E_{in} = \eta_T \cdot T \cdot E_L$. Whereas these losses, which are in the order of 20% overall, affect the fluence in orbit via the transmitted laser energy, the impact atmospheric turbulence comes into play with the spot size. If not compensated for, beam broadening yields a significantly larger spot, cf. Fig. 2 in [18] for this particular laser configuration, which significantly reduces the fluence in the focal area at the debris position. In this case the spot radius can be computed using

$$\boldsymbol{r_{s,turb} = \sqrt{\left(\frac{M^2 \lambda\, z(\zeta, h)}{\pi\, w_0}\right)^2 + 8\left(\frac{\lambda\, z(\zeta, h)}{\pi\, r_0(\zeta)}\right)^2 \cdot \left(1 - 0.26 \cdot \sqrt[3]{\frac{r_0(\zeta)}{w_0}}\right)^2}} \tag{3}$$

where $r_0(\zeta)$ is the spherical wave coherence diameter for up-links, derived from integration of the turbulence strength C_n^2 over all atmospheric layers [19]. It can be seen from Fig. 3b) that, together with the transmission losses outlined above, uncompensated turbulence would lower the fluence in orbit by more than one order of magnitude, rendering laser ablation impossible for the analyzed laser configuration.

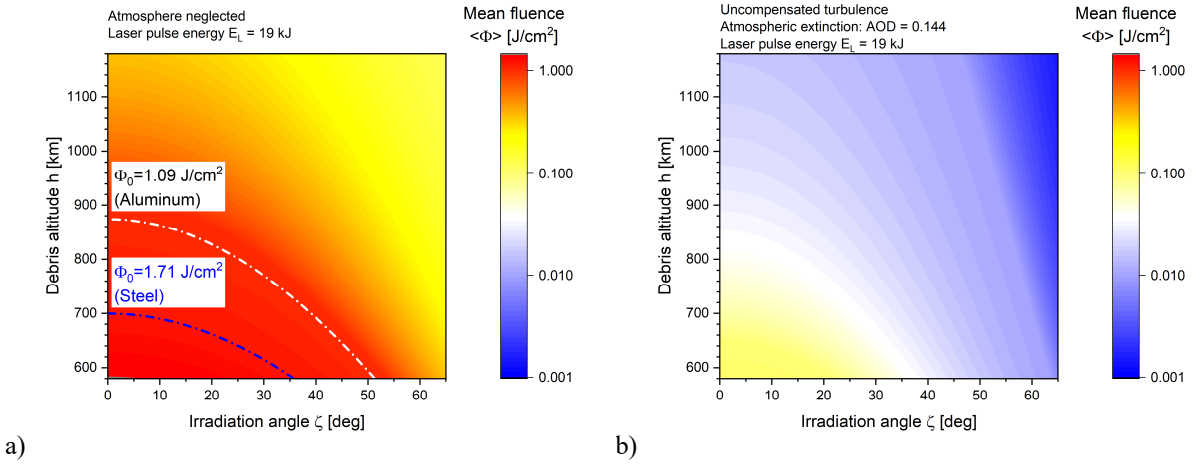

a) b)

Fig. 3. Average laser fluence of the focus spot in orbit from beam transmission by a ground station with 2.5 m aperture using a laser wavelength of $\lambda = 1053\ nm$ and a beam quality parameter of $M^2 = 2.25$.

Hence, it is obvious that the compensation of turbulence-induced beam broadening by adaptive optics is a mandatory prerequisite to achieve laser ablation at a space debris target. Moreover, it can be seen that even in the

idealized case of undisturbed beam propagation the ablation threshold of the targeted materials would hardly be exceeded, cf. Fig. 2. At the given constraints of $\lambda = 1053\ nm$ and $M^2 = 2.25$ this demands for the usage of a larger laser pulse energy, which in the following is accounted for by assuming beam coupling of 4 laser beamlines yielding overall $E_L = 76\ kJ$. Regarding the spot size, we propose the usage of an adaptive optics system like the one described in [3], comprising a deformable mirror with a bandwidth $f_{3dB} = 300\ Hz$ together with 300 actuators for the named mirror in order to dynamically modify the wavefront of the emitted laser beam based on the measured deformation of the wavefront of the light received from an artificial laser guide star slightly ahead the debris position. Then, the turbulence-compensated beam radius $r_{s,ao} = r_{s,vac}/\sqrt{Str}$ is significantly smaller [18] and fluences which are comparable to the case of undisturbed beam propagation can be achieved, cf. Fig. 4. The computation of the respective Strehl ratio $Str = Str(\zeta, h)$ is lined out in greater detail in [3].

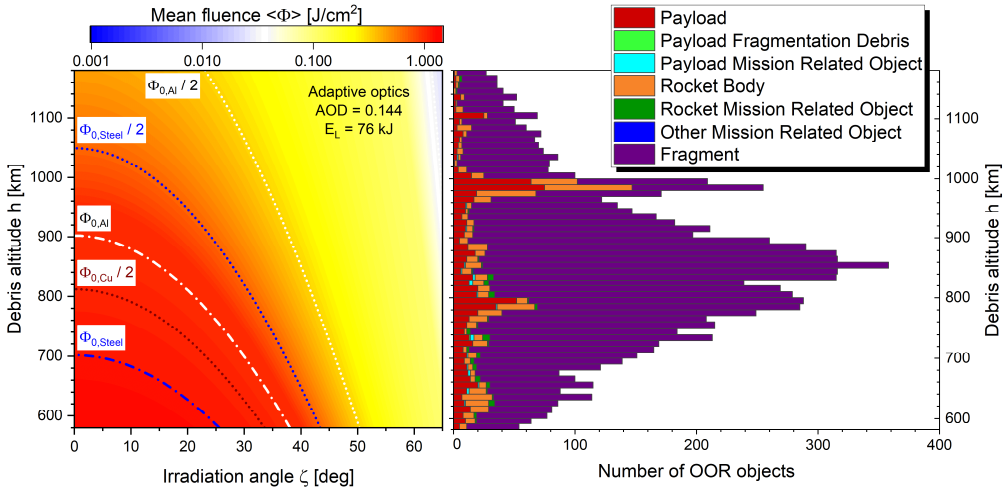

Fig. 4. Mean fluence in orbit using adaptive optics and four laser beamlines ($E_L = 76\ kJ$), together with OOR debris population as a function of mean orbital altitude. Threshold fluences for laser ablation are marked with dash-dotted lines in the fluence graph. Dotted lines indicate where 50% of the threshold fluence is surpassed which is equivalent to the ablation threshold in the center of a spot with Gaussian fluence distribution.

4.2 Momentum from Laser Ablation

In a first, high-level comparison [18] between laser ablation and photon pressure for debris orbit modification we used the mean fluence $\langle\Phi\rangle$ as outlined above to derive momentum from laser-ablative recoil in comparison with laser photon pressure for representative OOR sample targets. In this simplified assumption about the laser fluence, however, momentum is discarded in many irradiation settings where the average fluence falls below the threshold fluence for laser ablation ($\langle\Phi\rangle < \Phi_0 \rightarrow \Delta p = 0$) but the peak fluence in the center does not ($\Phi_{peak} = 2 \cdot \langle\Phi\rangle > \Phi_0 \rightarrow \Delta p > 0$, assuming a Gaussian fluence distribution in the focus). Here, for a better assessment of the imparted momentum we use

$$\Delta \boldsymbol{p} = \int \boldsymbol{c_m}\big(\boldsymbol{\Phi}(\vec{\boldsymbol{r}})\big) \cdot \boldsymbol{\Phi}(\vec{\boldsymbol{r}})\, \boldsymbol{dA} = \boldsymbol{2\pi} \int_{\boldsymbol{0}}^{\boldsymbol{r_0}} \boldsymbol{c_m}\big(\boldsymbol{\Phi}(\boldsymbol{r})\big)\boldsymbol{\Phi}(\boldsymbol{r})\boldsymbol{r}\, \boldsymbol{dr} \tag{4}$$

where $\Phi(r) = 2E_{in}/(\pi r_s^2) \cdot exp(-2\,r^2/r_s^2)$ and r_0 denotes the radius of the area inside the focused laser spot where ablation can effectively take place. From this, the imparted in-track momentum can be computed using the projection on the actual tangent on the object's trajectory via $\Delta p_i = \Delta p \cdot \cos\beta$. The respective results are shown in Fig. 5 for the different target materials of this study. It can clearly be seen that the onset of momentum generation is located at combinations of altitude and zenith angle where $\langle\Phi\rangle$ exceeds $\Phi_0/2$, cf. the dotted lines in Fig. 4. Moreover, momentum coupling to aluminum outperforms steel which, in turn, significantly outperforms copper as a target surface material. For this configuration of laser and transmitter, debris at higher altitudes > 1050 km is only accessible for laser ablation with aluminum as surface material while a copper surface would even limit the upper altitude for ablation down to approximately 800 km. Regarding the beam pointing elevation, small zenith angles ζ

are associated with relatively short distances between transmitter and debris and, hence, with higher fluences. However, a low value for ζ is rather detrimental for irradiation in terms of the in-track component of imparted momentum which decreases with increasing β. As a trade-off between target distance and in-track projection, an irradiation angle in the order of $\zeta = 20° \ldots 30°$ yields the highest velocity change of the debris object here. Note that due to the strong non-linearity of momentum coupling, cf. Fig. 2, these findings cannot be generalized but have to be derived for every combination of laser, transmitter, and target surface material specifically.

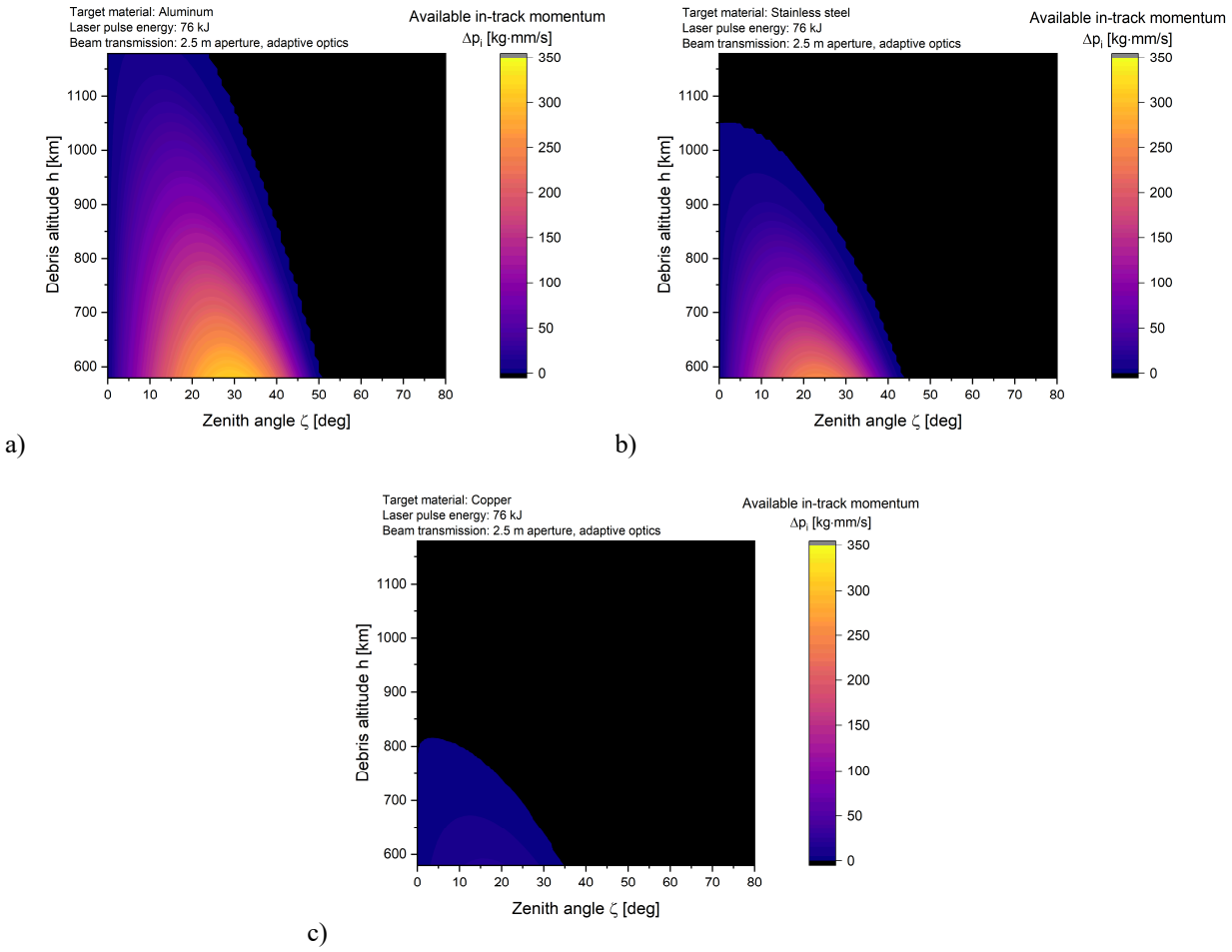

Fig. 5. Assessment of available in-track momentum from laser-ablation for debris targets with a) aluminum, b) stainless steel, and c) copper as surface material.

For various reasons the computed in-track momentum shown in Fig. 5 constitutes more or less an upper limit of possible momentum: For example, if the target size is smaller than the laser spot area in which ablation is possible, outshining losses occur which diminish the imparted momentum. Moreover, if the laser beam is not oriented perpendicular to the target surface the incident fluence will be lower and, for the fluence regime considered here, the momentum coupling coefficient will be smaller as well. Only at very high fluences beyond the optimum fluence for momentum coupling a lowered fluence might be beneficial instead.

In order to assess the impact of outshining losses and target orientation, we have carried out Monte Carlo simulations for all 9101 debris targets of our study, cf. Sect. 3.2, which cover a wide range of object masses and sizes. For the simulations described in this section, we have used our raytracing-based code EXPEDIT computing Monte Carlo samples of laser-ablative momentum for arbitrary target orientations. At least 11 samples (maximum: 1000) have been calculated for each target, and computations had been terminated when the results of the imparted momentum reached a certain criterion for convergence (accuracy of the 95% confidence interval of the results

falling below 10% of their average value). The respective results are plotted in Fig. 6 as a function of the debris orbital altitude. It can clearly be seen that the consideration of target size yields a significantly smaller predicted momentum compared to the analytical results of Fig. 5, which are represented by the green line in Fig. 6. Moreover, the impact of the debris size on momentum can evidently been associated with the debris category: Outshining losses are the most pronounced for the small fragments whereas they are rather moderate for payloads and, in particular, rocket bodies, cf. the average optical cross-sectional areas of those target categories given in Table 2.

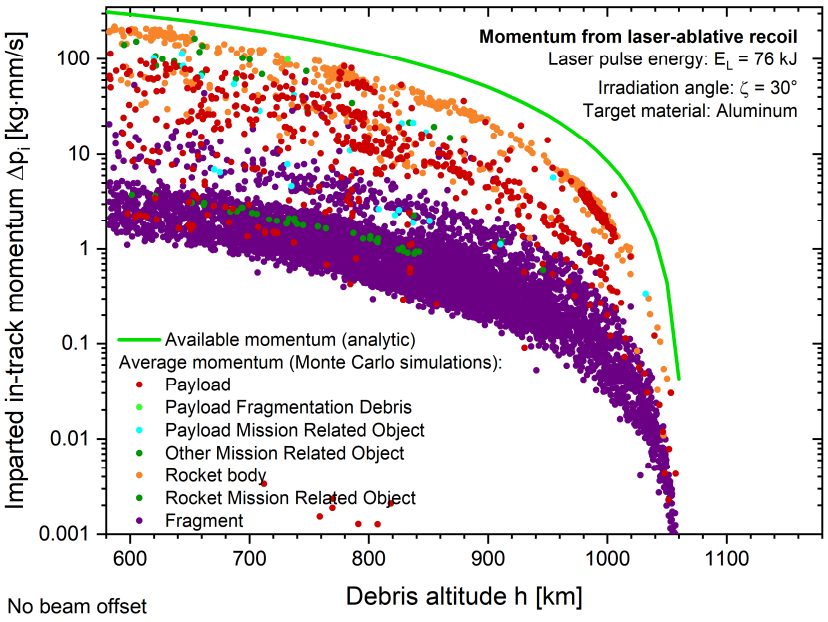

Fig. 6. Mean imparted momentum available from a laser pulse of $E_L = 76\ kJ$ at an irradiation angle of $\zeta = 30°$ as a function of debris altitude. Findings from analytical considerations as of Fig. 5 in comparison to results from Monte Carlo simulations considering debris shape and random orientation.

Beyond the prediction uncertainty in laser-imparted momentum due to limited knowledge of the object's shape and orientation, uncertainty about the beam offset against the debris center of mass comes into play due to residual errors in beam pointing together with the available tracking uncertainty. If the target, however, is not hit by the spot center but rather by its outer regions, smaller fluences will be available for momentum generation only, which aggravates the losses in momentum in addition to the outshining losses arising from spatial mismatch. For a quantitative assessment, we have introduced two additional degrees of freedom to our Monte Carlo simulations using a hit uncertainty σ_r modeled as Gaussian probability distribution of beam center offset against the target's center of mass stemming from a tracking uncertainty of $\sigma_t = 0.1"$ (assuming adaptive optics usage for downlink) and a residual pointing uncertainty of $\sigma_p = 0.01"$ yielding $\sigma_r = \sqrt{\sigma_t^2 + \sigma_p^2}$, cf. [3]. As can be seen from the ratio q_{vi} given in Table 2, the resulting momentum from laser ablation is lower than in the case of beam pointing with ultimate precision, i.e., no beam offset.

Table 2. Object number, average mass m and average optical cross-sectional area A_{cs} for the debris targets investigated in this study. q_{vi} gives the ratio of laser-ablative momenta for the case of 0.1" tracking uncertainty vs. the case of no beam offset against the target's center of mass.

Debris category	*Number*	$m\ [kg]$	$A_{cs}\ [m^2]$	$q_{vi}[-]$
Rocket bodies	606	1480 ± 1521	12.2 ± 8.5	0.89 ± 0.13
Payloads	770	631 ± 751	4.0 ± 5.6	0.75 ± 0.13
Mission-related objects	90	49 ± 111	1.8 ± 3.2	0.74 ± 0.14
Fragments	7635	5 ± 61	0.02 ± 0.19	0.58 ± 0.14

4.3 Debris Displacement

Since the imparted laser-ablative momentum strongly depends from the irradiation conditions we have analyzed different beam elevations with respect to the imparted momentum. Recoil from laser ablation has been computed in our Monte Carlo analyses for different zenith angles by 5° steps ($\zeta = 0°, 5°, 10° \ldots \zeta_{max}$) where ζ_{max} is the maximum angle (modulo 5°) for which ablation can be achieved, i.e., $\langle\Phi\rangle(\zeta, h) > \Phi_0/2$. Subsequently, the optimum irradiation angle ζ_{opt} maximizing the imparted in-track velocity change Δv_i has been determined for each debris target individually. It can be seen from Fig. 7 that the optimum irradiation angle ζ_{opt} comes from the abovementioned trade-off between a rather large angle which implies a greater contribution of the imparted momentum to the in-track velocity change and, on the other side, a rather small zenith angle yielding a smaller laser spot size and, correspondingly, a high laser fluence, which gives a larger overall momentum. The latter issue is pronounced in particular for materials exhibiting a comparatively high fluence threshold for ablation as well as for targets at higher orbit altitudes. Higher pulse energies, however, would shift ζ_{opt} towards larger values which eventually results in a better efficiency in terms of the required in-track projection of the imparted momentum.

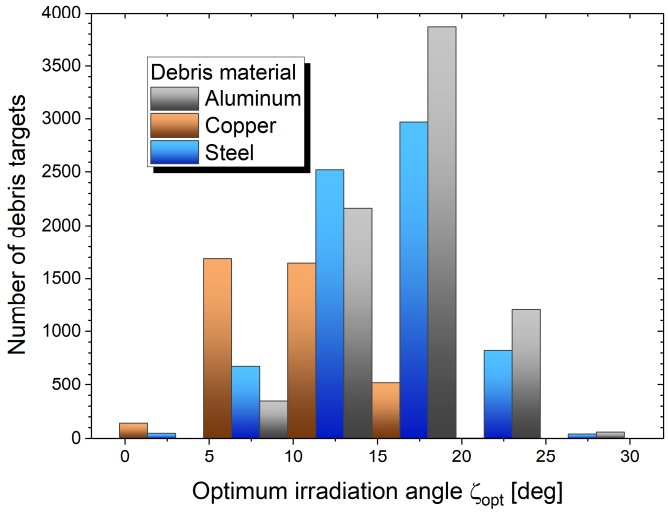

Fig. 7. Optimum zenith angle for laser irradiation of space debris targets of different materials with $E_L = 76\ kJ$ laser pulse energy, $\sigma_t = 0.1$" tracking uncertainty, and $\sigma_p = 0.01$" beam pointing precision.

Analyzing the momentum imparted from a high energy laser beam pointed to the target under its optimum zenith angle, it can be seen from

Fig. 8 that only for a minority of targets an in-track velocity change can be achieved by a single pulse which would be necessary to yield a 2σ displacement after 24 hours corresponding to the average in-track uncertainty in a laser tracking network, i.e., $\Delta v \geq \Delta v_{LXN}$. If, however, the uncertainty directly after a laser ranging measurement was considered a relevant feasibility criterion, i.e., $\Delta v \geq \Delta v_{LT,0}$, collision avoidance would be deemed feasible for the majority of fragments and a significant number of rocket bodies and payloads, unless the object is relatively small or its mass exceeds approximately 1000 kg. In general, the dependency of imparted momentum from the target's surface material can clearly be seen and the upper altitude limit for momentum generation clearly corresponds with the material's ablation threshold Φ_0. Apart from these limitations, nevertheless, it has to be highlighted that for aluminum debris at low OOR altitudes the imparted velocity change exceeds the respective Δv_i from photon pressure from laser irradiation at a power level of 40 kW (CW) during a few minutes of a station transit while $15° \leq \zeta \leq 65°$, cf. [3], by up to more than one order of magnitude.

Regarding the feasibility criteria of collision avoidance introduced in Sect. 2, it has already been shown in Table 2 that the imparted momentum and, hence, feasibility of collision avoidance depends from the uncertainty of orbital data. Whereas $\Delta v_{LT,0}$ and Δv_{LXN} are general thresholds for the imparted velocity change, target-specific thresholds have been introduced as well in Sect. 2 which refer to the target size (Δv_{dim}) and its orbital altitude ($\Delta v_{LT,24}^{(2\sigma)}$),

respectively. Here, a feasibility ratio can be defined by comparison of the imparted velocity increment Δv_i with the respective feasibility threshold. The corresponding results, shown in Fig. 9, indicate that in the idealized best-case scenario, in which the debris position at TCA can be predicted exactly 24 h in advance and, hence, Δv_{dim} would make sense, collision avoidance would be feasible for nearly all OOR objects up to a size of 4 meters, cf. Fig. 9.a). If, however, a laser ranging measurement of minimum 24 h before TCA and subsequent orbit propagation would be used for determination of the debris position at TCA, collision avoidance would only be deemed feasible for very few objects, cf. Fig. 9.b). Presumably the true potential of laser-ablative collision avoidance lies somewhere in between these extreme feasibility assessments. Hence, for more advanced studies on laser-based collision avoidance, analysis of the changes of collision probability instead of orbital velocity changes [5] would be a more sound and practical method.

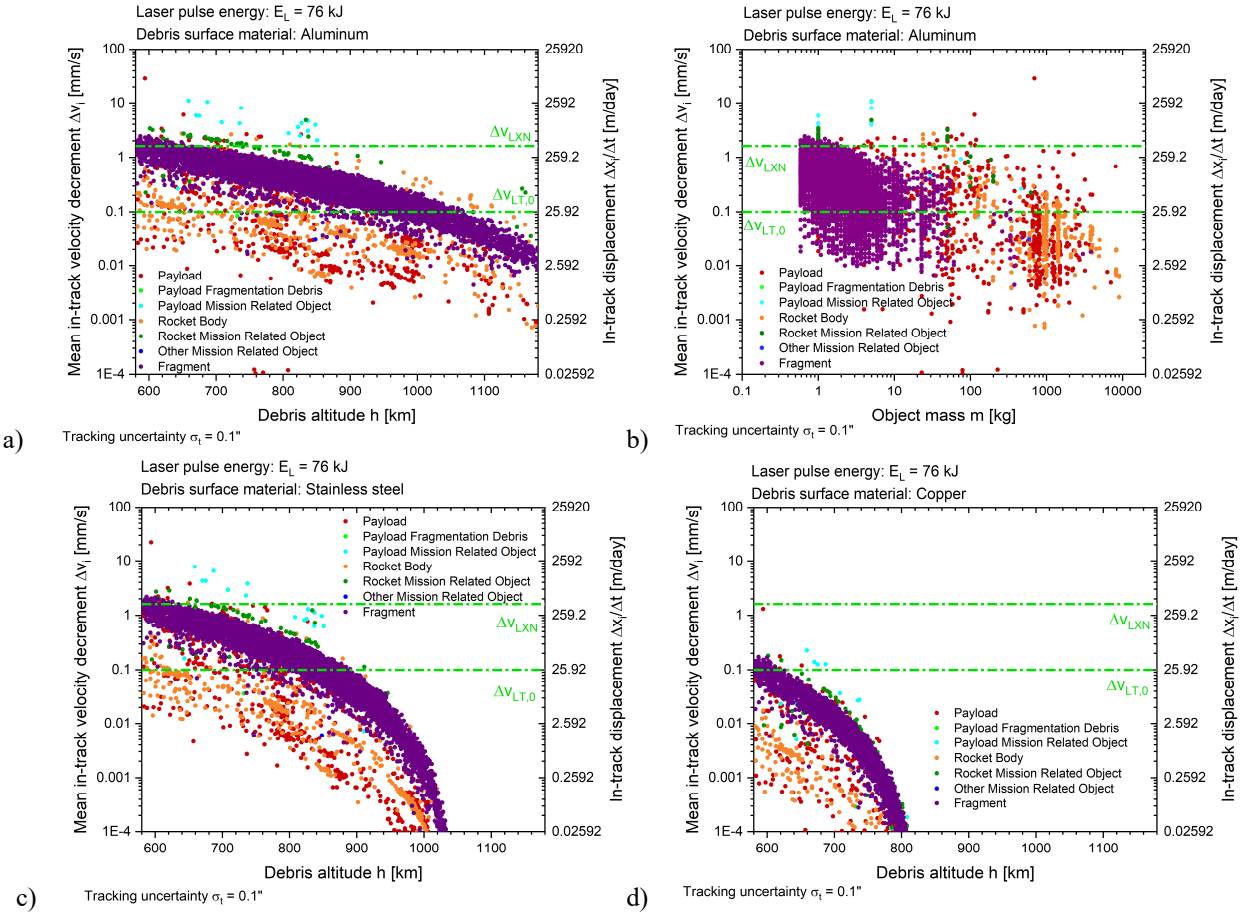

Fig. 8. Mean in-track velocity decrement from laser ablative recoil under irradiation with a ground-based laser site emitting a single laser pulse of 76 kJ pulse energy. Target materials are aluminum (Figs. a) and b)), stainless steel (c), and copper (d), respectively. Results have been derived from Monte Carlo simulations averaging over samples with random target orientation and beam offset in laser pointing using a tracking uncertainty of 0.1 arcsec. For each target the optimum zenith angle is chosen where Δv_i takes its maximum value.

4.4 Collision Avoidance Success Probability

In the considerations above, only the average of the imparted momentum has been used, which comes from statistics covering all Monte Carlo samples for a given target under arbitrary orientation and random offset to the laser beam center. In a real scenario, however, only a single laser pulse would be applied during the transit, which equals a single Monte Carlo sample. Depending on orientation and offset, however, the imparted momentum can vary

greatly. Therefore, the results for Δv_i from the Monte Carlo sample sets for each debris target have been analyzed with respect to the different feasibility criteria Δv_{feas}. Here, we define the success probability p_{CA} of collision avoidance by the ratio of the number of samples where Δv_i exceeds the feasibility threshold to the number of all Monte Carlo samples N_s for a given target, which is in the order of a few hundred samples (averaged over all simulations: 628 ± 286):

$$\boldsymbol{p_{CA} = \frac{N\left(\Delta v_i > \Delta v_{feas}\right)}{N_s}}. \tag{5}$$

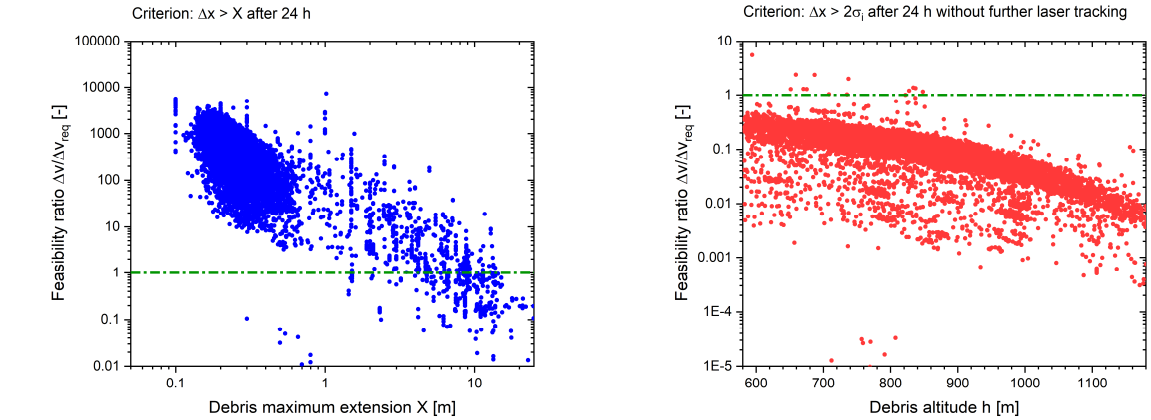

a) b)

Fig. 9. Feasibility assessment of laser-ablative collision avoidance with a single pulse using different criteria: a) object size and b) in-track uncertainty 24 h after a laser ranging measurement. Target material: aluminum.

The corresponding results for our simulations are shown in Fig. 10. It can be taken from the graph that the success probability exceeds 50% only for a few objects when typical uncertainties of orbital data based on orbit propagation after a laser ranging measurement are considered. Nevertheless, at the least a 25% chance of success is already given for a few hundred objects under these constraints. Acknowledging, however, that for the majority of targets successful collision avoidance would likely be successful if a very high precision of the position of TCA was available, the proposed approach for single-pulse collision avoidance appears promising regarding future advances in space situational awareness.

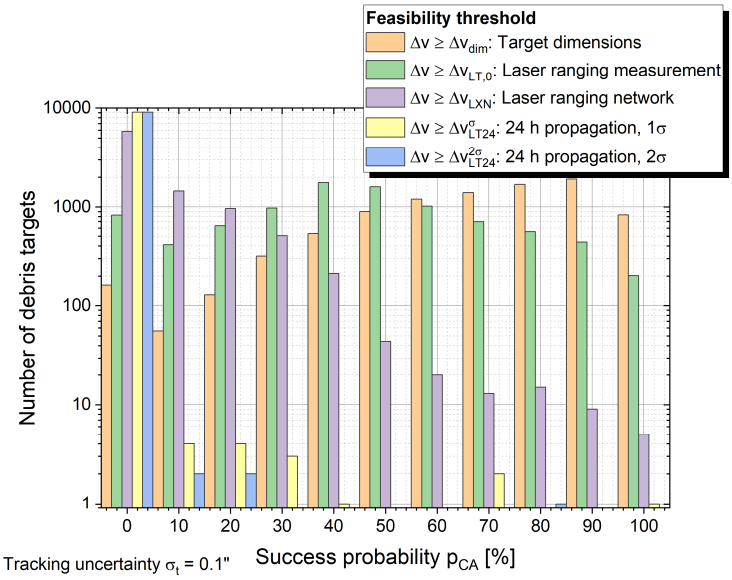

Fig. 10. Histogram on success probability of single-pulse (76 kJ) laser-based collision avoidance for different feasibility criteria, cf. Sect. 2.

5. CONCLUSIONS AND OUTLOOK

The main striking issue in this analysis might be found in the very large laser pulse energies used in our computations in contrast to other configurations in the literature [9][10]. In [9], for example, selection of a shorter wavelength, $\lambda' = 530\ nm$, and a larger transmitter aperture, $D_T{}'$ would already yield a significant increase of the fluence in orbit by more than one order of magnitude, regardless of the Strehl performance of the respective adaptive optics. In our study, however, we abstain from the beneficially shorter wavelengths of visible laser light regarding atmospheric scattering and related light pollution, dazzling on ground and in particular of air traffic and corresponding public awareness and concerns. In addition to that, our assumption on laser beam quality, $M^2 = 2.25$, can be deemed rather conservative, since only departing from the pre-existing beamlines exhibiting a rectangular beam profile. In further course research and development, usage of a Gaussian beam profile might yield a significantly better beam quality $M^2 < 1.5$. Moreover, we restrain here to a rather small aperture diameter of $D_T = 2.5\ m$ acknowledging that for $D_T > 4\ m$ tiled apertures would be needed, which, in contrast to monolithic transmitters, exhibit a relatively high risk of thermal damage due to laser induced heat.

With space debris maneuvering by photon pressure, the main scope of beam focusing is not to lose laser energy by outshining the target. The imparted momentum itself, however, does not change with the spot size as long as the target is hit and geometric effects from the debris shape can be neglected. In laser ablation, however, the laser spot size is crucial since it affects the incident fluence that has to be significantly higher than the material-specific threshold of the ablation process. Therefore, compensation of turbulence-induced beam broadening by high-end adaptive optics systems technology is mandatory.

In sum, the findings of our study support the conceptual approach that, at least for low altitudes up to 880 km, already a *single* laser station capable of just single-pulse operation but exhibiting a laser pulse energy of approximately 80 kJ to remotely induce laser ablation might have a similar potential for space debris collision avoidance like a global network of *ten* laser stations for MT by photon pressure with 40 kW laser power each, as proposed in [5].

Admittedly, high energy lasers beyond the 10 kJ pulse energy level can currently only be found at research institutes for fusion experiments whereas high power CW lasers, suitable to exert laser force by photon pressure, are commercially available. In the long run, however, a single multi-kJ laser might constitute be an attractive stand-alone alternative to a network of high-power CW laser stations – or a useful supplementary device in a hybrid (CW + pulsed) framework for collision avoidance.

Finally, regarding the large amount of laser pulse energy being instantaneously released in orbit, ($E_L = 76\ kJ$ is equivalent to 18.2 grams of TNT (trinitrotoluene) explosive), the question of responsible use and conceivable misuse should be addressed aiming for a global governance of such systems, e.g., as lined out in [20], in order to tackle the global challenge of collisions with space debris.

6. ACKNOWLEDGMENTS

The usage of USSTRATCOM catalogue of TLE data, the ESA DISCOS database as well as ESA's MASTER-8 debris population model is thankfully appreciated. The scientific discussions with our colleagues from the LARAMOTIONS study – Heiko Dreyer, Paul Wagner, Ewan Schafer, Urs Hugentobler, Christoph Bamann, Pawel Lejba, Tomasz Suchodolski, Egon Döberl, Dietmar Weinzinger, and Wolfgang Promper – and the related project supervisory group at ESA – Tim Flohrer, Srinivas Setty, Andrea Di Mira, Igor Zayer, and Emiliano Cordelli – are thankfully acknowledged as well as the work of Jascha Wilken and Lukas Eisert on development of the numerical code EXPEDIT.

7. REFERENCES

[1] J. Mason et al., "Orbital debris-debris collision avoidance," *Advances in Space Research* 48, 1643 – 1655 (2011).
[2] C.R. Phipps et al., "Removing orbital debris with lasers," *Advances in Space Research* 49, 1283 – 1300 (2012).

[3] S. Scharring et al., "LARAMOTIONS: A conceptual study on laser networks for near-term collision avoidance for space debris in the low Earth orbit," *Applied Optics* (submitted for publication).
[4] C. Bamann et al., "Analysis of collision avoidance via ground-based laser momentum transfer," *Journal of Space Safety Engineering* 7, 312 – 317 (2020).
[5] H. Dreyer et al., "Future improvements in conjunction assessment and collision avoidance using a combined laser tracking/nudging network," in: *8th European Conference on Space Debris*, paper 153 (2021).
[6] C. Phipps et al., "Review: Laser-Ablation Propulsion," *Journal of Propulsion and Power* 26(4), 609 – 637 (2010).
[7] R.-A. Lorbeer et al., "Experimental verification of high energy laser-generated impulse for remote laser control of space debris," *Scientific Reports* 8, 8453 (2018).
[8] H. Krag et al., "Ground-Based Laser for Tracking and Remediation – An Architectural View," in: *69th International Astronautical Congress*, paper IAC-18-A6.7.1 (2018)
[9] C.R. Phipps et al., "Orion: Clearing Near-Earth Space Debris Using a 20 kW, 530 nm, Earth-Based, Repetitively Pulsed Laser," *Laser and Particle Beams* 14(1), 1 – 44 (1996).
[10] A.M. Rubenchik et al., "Laser Systems for Orbital Debris Removal," *AIP Conference Proceedings* 1278, 347 – 353 (2010).
[11] C.A. Haynam, "National Ignition Facility laser performance status," *Applied Optics* 46(16), 3276 – 3303 (2007).
[12] CEA – Direction des Applications Militaires, "Laser Mégajoule: Description de l'installation LMJ," http://www-lmj.cea.fr/lmj-description.html (last access: July 16, 2021).
[13] J.N. Opiela, "A study of the material density distribution of space debris," *Advances in Space Research* 43, 1058 – 1064 (2009).
[14] B.C. D'Souza, "Development of impulse measurement techniques for the investigation of transient forces due to laser-induced ablation," PhD thesis, University of Southern California (2006).
[15] S. Scharring et al., "Momentum predictability and heat accumulation in laser-based space debris removal," *Optical Engineering* 58(1), 011004 (2018).
[16] N. Hodgson and H. Weber, "Laser Resonators and Beam Propagation," 2nd ed., Springer (2005).
[17] R.A. McClatchey et al., "Optical properties of the atmosphere," Air Force Cambridge Research Laboratories (1972).
[18] S. Scharring et al. "Potential of using ground-based high-power lasers to decelerate the evolution of space debris in LEO," in: *8th European Conference on Space Debris*, paper 98 (2021).
[19] R.L. Fante, "Electromagnetic beam propagation in turbulent media," Proc. IEEE 63, 1669–1692 (1975)
[20] P. Bohacek, "Responsible Use of Lasers in Space," published at UN Office of Disarmament (2021), available online at: https://www.un.org/disarmament/topics/outerspace-sg-report-outer-space-2021/